

Impact-Analysis for Coexisting G.fast and Vectored VDSL2

Daniel Hincapie and Gerhard Maierbacher

Fraunhofer Institute for Embedded Systems and Communication Technologies ESK, Hansastrasse 32, D-80686 Munich, Germany

Email: {daniel.hincapie, gerhard.maierbacher}@esk.fraunhofer.de

Abstract—G.fast recently standardized by the ITU [1] aims at providing gigabit access from the Distribution Point (DP). The deployment of this new technology will be progressive as previous technological migrations, so G.fast will share the access network with existing DSL systems, particularly with vectored VDSL2. However, G.fast and vectored VDSL2 as defined by the standards are spectral-incompatible due to their overlapping spectrum, different carrier spacing implementation and conflicting multiplexing schemes. This work analyzes the coexistence issues that arise when G.fast and vectored VDSL2 services are deployed from the DP. Potential gains that could be obtained by introducing a synchronized transmission scheme, as well as the effectiveness of spectral-compatible band plans are discussed in order to help determine if those measures should be developed further and/or considered for standardization. In order to achieve this goal, we establish far-end crosstalk (FEXT) and near-end crosstalk (NEXT) models for realistic simulations and analyze the system performance for different deployment scenarios that reproduce the progressive migration from VDSL2 to G.fast. Our results show that synchronization between vectored VDSL2 and G.fast barely improves their performance, whereas the deployment of spectral-compatible band plans is an effective means to improve vectored VDSL2 performance with tolerable impact on G.fast.

I. INTRODUCTION

G.fast is the most recent generation of digital subscriber line (DSL) standards envisioned to provide gigabit internet access from the distribution point (DP). By widening the spectrum up to 212 MHz, and increasing the symbol rate and carrier spacing used in former DSL standards [1], G.fast is able to potentially provide up to 2 Gbps of aggregate data rate from the DP [2]. In addition, G.fast has incorporated time domain duplexing (TDD) to offer flexible definition of upstream and downstream data rates.

Although G.fast is a promising technology, it will be introduced gradually in today's access network. Service providers expect to safeguard their former technological investments and meet some clients' willingness of not upgrading their current broadband service. Therefore, G.fast systems will share the network infrastructure with existing systems, particularly with vectored very-high-bit-rate DSL 2 (VDSL2) [3], [4] due to

their presence in the same access network segment, i.e., fiber-to-the-distribution-point (FTTdp) and fiber-to-the-curb (FTTC) share the same binder cable. However, the technological changes incorporated in G.fast make it spectral-incompatible with vectored VDSL2 as their spectra overlap; G.fast uses the frequency band between 2.2 MHz and 212 MHz [1], whereas VDSL2 uses frequencies up to 30 MHz [3]. The impact on VDSL2 is mitigated reducing the transmitted power spectrum density (PSD) and the aggregate power of G.fast systems [1]. Furthermore, spectral-compatible G.fast band plans limited to only use frequencies above 17 MHz have been considered [1]. Despite of these mitigation approaches, the spectral incompatibility persists due to four aspects: the noticeable difference between their bandwidths, the implementation of different carrier spacing, the asynchronous symbol transmission and the use of different multiplexing schemes. The first aspect implies that received symbols are sampled using different sampling rates after transceivers' anti-aliasing filtering stage. This, in combination with the different carrier spacing and asynchronous transmission, conveys inter-carrier interference (ICI) between coexisting systems [5], [6]. Regarding the multiplexing schemes, G.fast implements TDD whereas VDSL2 uses frequency-division duplexing (FDD). Therefore, there is not spectral separation between upstream and downstream transmissions in G.fast, so its receivers are interfered by counterpart's transmitters at the far-end, i.e., far-end crosstalk (FEXT), as well as at the near-end, i.e., near-end crosstalk (NEXT). In the same sense, VDSL2 receivers are exposed to FEXT and NEXT crosstalk. However, the interfering sources for VDSL2 are bursting as G.fast transmitters are only active during assigned upstream and downstream time slots. Such a hostile interference environment poses a challenging scenario for the rollout of G.fast services, turning the performance analysis of coexisting vectored VDSL2 and G.fast into a hot topic for service providers, academia and standardization bodies.

In this work, we study the mutual impact between vectored VDSL2 and G.fast systems in downstream transmission when jointly operated from the DP. For our analysis, we select different VDSL2/G.fast deployment scenarios to represent the progressive migration from VDSL2 to G.fast. We then estimate the potential benefits of establishing synchronous transmission

This work has been partially financed by the research project "FlexDP-Flexible Breitband Distribution Points", funded by the Bayerische Forschungsstiftung (Bavarian Research Foundation).

between VDSL2 and G.fast and analyze spectral-compatible band plans as a means to minimize the impact of G.fast on vectored VDSL2 performance. In order to achieve this goal, we first analyze empirical measurements to develop NEXT and FEXT models for the G.fast frequency range. To ensure a realistic simulation setup, we use the length distribution considered in [7] and the loop lengths studied in [8], [9] to reproduce the DP topology.

The rest of this paper is organized as follows: Section II presents the system model and the vectoring scheme implemented to simulate G.fast and VDSL2 systems. Section III describes the approach and results of the stochastic FEXT and NEXT models and their characterization for a commonly used 50-pair cable. Section IV exposes the characterization of the access network. Section V defines the simulation scenarios and presents performance results and comparative analysis for different degrees of G.fast deployment. Concluding remarks are given in Section VI.

II. SYSTEM MODEL

We consider a DSL network with N users and K frequency sub-carriers. The DSL channel, i.e., the binder cable, is characterized by FEXT and NEXT channel matrices $\mathbf{H}_k^{\text{FEXT}}$, $\mathbf{H}_k^{\text{NEXT}} \in \mathbb{C}^{N \times N}$.

A. Synchronous and asynchronous transmission

Using synchronous discrete multi-tone (DMT) modulation, same sampling rate and carrier spacing, there is no ICI [10] and the transmission over each sub-carrier k can be independently modeled as

$$\mathbf{y}_k = \mathbf{H}_k^{\text{FEXT}} \cdot \mathbf{x}_k^{\text{FE}} + \mathbf{H}_k^{\text{NEXT}} \cdot \mathbf{x}_k^{\text{NE}} + \mathbf{z}_k, \quad (1)$$

where $\mathbf{x}_k^{\text{FE}} = [x_k^{1,\text{FE}}, \dots, x_k^{N,\text{FE}}]^T$, $\mathbf{x}_k^{\text{NE}} = [x_k^{1,\text{NE}}, \dots, x_k^{N,\text{NE}}]^T$, $\mathbf{y}_k = [y_k^1, \dots, y_k^N]^T$ and $\mathbf{z}_k = [z_k^1, \dots, z_k^N]^T$ represent the signal transmitted by the far-end (FE) transmitter, the signal transmitted by the near-end (NE) transmitter, the received signal and the total additive noise for users $1 \dots N$ on sub-carrier k , $1 \leq k \leq K$, respectively. $[\mathbf{H}_k]_{(n,m)} = h_k^{(n,m)}$ is the channel gain from transmitter m to receiver n on sub-carrier k . The insertion losses of direct channels are given by the main diagonal elements $\text{diag}(\mathbf{H}_k^{\text{FEXT}}) = h_k^{\text{FEXT}(n,n)}$, whereas its out-of-diagonal elements $h_k^{\text{FEXT}(n,m)}$ for $n \neq m$ correspond to the interfering FEXT channel gains. Out-of-diagonal elements of $\mathbf{H}_k^{\text{NEXT}}$, i.e., $h_k^{\text{NEXT}(n,m)}$ for $n \neq m$, correspond to the interfering NEXT channel gains, and its diagonal elements are the direct channels' return loss. The transmit PSD of user n on sub-carrier k is $s_k^n = \mathcal{E}\{|x_k^n|^2\}/\Delta_f$, where Δ_f is the sub-carrier bandwidth [10].

The number of bits that can be transmitted at an arbitrary low bit error rate (BER) by user n on sub-carrier k is

$$b_k^n \triangleq \log_2 \left(1 + \frac{1}{\Gamma} \frac{|h_k^{n,n}|^2 s_k^n}{\chi_k^{\text{sync},n} + \sigma_k^n} \right), \quad (2)$$

where

$$\chi_k^{\text{sync},n} = \underbrace{\sum_{\substack{m=1 \\ m \neq n}}^N |h_k^{n,m,\text{FEXT}}|^2 s_k^{m,\text{FE}}}_{\text{FEXT noise power}} + \underbrace{\sum_{\substack{m=1 \\ m \neq n}}^N |h_k^{n,m,\text{NEXT}}|^2 s_k^{m,\text{NE}}}_{\text{NEXT noise power}}, \quad (3)$$

is the aggregate crosstalk power for synchronized DMT symbol transmission, Γ is the Shannon gap and $\sigma_k^n \triangleq \mathbb{E}\{|z_k^n|^2\}/\Delta_f$ is the total additive noise PSD of user n on sub-carrier k with sub-carrier bandwidth Δ_f . Therefore, the achievable data rate R for user n is $R^n = f_s \sum_{k=1}^K b_k^n$, where $f_s \leq \Delta_f$ is the symbol rate of the system.

If systems asynchronously transmit DMT symbols with different band width, carrier spacing and sampling rate, there is ICI [11]. Under ICI, the aggregate crosstalk interference for asynchronous transmission $\chi_k^{\text{async},n}$ experienced by user n on tone k is [6]

$$\chi_k^{\text{async},n} = \sum_{\substack{m=1 \\ m \neq n}}^N \sum_{j=1}^N \gamma_{k,j}^{n,m} |h_j^{n,m,\text{FEXT}}|^2 s_j^{m,\text{FE}} + \sum_{\substack{m=1 \\ m \neq n}}^N \sum_{j=1}^N \gamma_{k,j}^{n,m} |h_j^{n,m,\text{NEXT}}|^2 s_j^{m,\text{NE}}, \quad (4)$$

where $\gamma_{k,j}^{n,m}$ represents the ICI coefficient from user m to user n , and from tone j to tone k . In our simulations, we use the full and worst-case alignment ICI coefficients calculated respectively in [11, eq.(5),eq.(7)] for the influence of VDSL2 in G.fast, and in [11, eq.(12),eq.(16)] for the influence of G.fast on VDSL2.

B. Vectoring

Let us consider a group of N synchronized DSL systems with the same sampling rate and carrier spacing. Therefore, the DMT transmission can be modeled as in (1). Furthermore, let us assume that they implement a multiplexing technique to completely separate downstream and upstream transmissions. Thus, receivers only experience FEXT interference (often called "self-FEXT") and NEXT power in (3) can be neglected [12]. The synchronized transmission allows us to consider each sub-carrier channel as an independent multiple input - multiple output (MIMO) channel. Therefore, sub-carrier-based pre- and post-compensation can be applied respectively to downstream and upstream signals to mitigate the interference caused by coexisting services within the same binder cable [12]. This concept is known as *vectoring*. We refer the reader to [10] for an extensive review of vectoring schemes.

For downstream pre-compensation, [13] proposes a near-optimal linear precoder called the diagonalizing precoder (DPC). The DPC has the form

$$\mathbf{y}_k = \mathbf{H}_k \cdot \left(\frac{1}{\beta_k^{\text{DPC}}} \cdot \mathbf{H}_k^{-1} \cdot \text{diag}(\mathbf{H}_k) \right) \cdot \mathbf{x}_k + \mathbf{z}_k,$$

$$\beta_k^{DP} = \max_n \sum_{m \in N} |[\mathbf{H}_k^{-1}]_{(n,m)} \cdot h_k^{m,m}|^2, \quad (5)$$

where β_k^{DP} is a scaling factor to ensure that the system meets the PSD mask constraints [10], [13]. The resulting system yields an effective bit capacity for sub-carrier k and user n of

$$b_k^n = \log_2 \left(1 + \frac{1}{\Gamma \cdot (\beta_k^{DP})^2} \frac{|h_k^{n,n}|^2 \cdot s_k^n}{\sigma_k^n} \right).$$

It must be noticed that only self-FEXT is mitigated by the vectoring operation. Therefore, the crosstalk interference generated by non-vectorized/asynchronous systems is given by (4) and considered as component of the the total additive noise power σ_k^n .

III. FEXT AND NEXT CHANNEL MODELS

The MIMO channel for each user is composed of one direct channel and $N - 1$ interfering/crosstalk channels. The direct channel is the insertion loss of the twisted pair connecting DSL access multiplexer (DSLAM) ports and CPEs. Models of the direct channel for frequencies up to 300 MHz have been have been described in [14]. The crosstalk channel is in general more complex to model and different approaches have been described in [4], [15]–[19]

A. Stochastic model

Interfering channels are described by their crosstalk gains, i.e., FEXT and NEXT transfer functions between pairs. The technical specification in [15] defines "1% worst case" FEXT and NEXT models empirically obtained from measurements of several cable types. These models offer a reference estimation of FEXT and NEXT channels, but are rather pessimistic; they do not reproduce the magnitude dispersion due to the relative position of interfering and interfered pairs [16]. In reality, services in adjacent pairs generate stronger crosstalk magnitude than those located farther away within the binder. To model this dispersion, known as *space selectivity*, the work in [16] extends the standardized model in [15] and proposes a stochastic model that defines the FEXT transfer function as

$$H_{stoch}^{\text{FEXT}}(f) = |H_{WC-FEXT}(f, d)| \cdot e^{j\varphi(f)} \cdot 10^{-0.05\chi^{\text{FEXT}}(f)}, \quad (6)$$

where $|H_{WC-FEXT}(f, d)|$ is the magnitude of the 1% worst-case model, f is the frequency in Hz, d is the coupling distance in meters, φ is a random variable uniformly distributed in the interval $[0, 2\pi]$, and $\chi(f)$ is a Gaussian random variable expressed in dB with mean $\mu_{dB}^{\text{FEXT}}(f)$ and standard deviation $\sigma_{dB}^{\text{FEXT}}(f)$. The latter models the FEXT magnitude dispersion.

Because the space selectivity depends on the pairs arrangement within the binder cable, the stochastic approach described in (6) requires the statistical characterization of $\chi(f)^{\text{FEXT}}$ for every binder. Earlier works provide characterization for different binder cables, e.g., [4], [16]–[18]. The model in (6) is based on the worst-case $H_{WC-FEXT}(f, d)$ standardized

in [15], which is appropriate for the VDSL2 frequency range [4], [16]–[18], i.e., up to 30 MHz. However, measurements in quad-structured cables show that the intra-quad crosstalk magnitude, which dominates the crosstalk power sum, is not well described by this worst-case model [19]. As a contribution of this paper, we present (for the first time) the FEXT and NEXT characterization for frequencies up to 300 MHz of a quad-structured cable with 50 pairs. In particular, for the cable of type A-2Y(L)50×2×0.4 (poly-ethylene isolated, 50 pairs, 0,4 mm). We use the stochastic approach in (6) to analyze crosstalk measurements and obtain suitable stochastic models for FEXT and NEXT.

Let us extend (6) to define the NEXT transfer function as

$$H_{stoch}^{\text{NEXT}}(f) = |H_{WC-NEXT}(f, d_i)| \cdot e^{j\varphi(f)} \cdot 10^{-0.05\chi^{\text{NEXT}}(f)}, \quad (7)$$

where $|H_{WC-NEXT}(f, d)|$ is the magnitude of the 1% worst case model [15], d_i is the interfered pair's length, and $\chi^{\text{NEXT}}(f)$ is a Gaussian random variable expressed in dB with mean $\mu_{dB}^{\text{NEXT}}(f)$ and standard deviation $\sigma_{dB}^{\text{NEXT}}(f)$.

B. Worst-case model

Obtaining a suitable worst-case model for the intra-quad FEXT and NEXT magnitude is crucial to conduct the characterization of $\chi^{\text{FEXT}}(f)$ and $\chi^{\text{NEXT}}(f)$. In general, the worst-case crosstalk models defined in [15] can be described as

$$H_{XT} = K_{XT} \times F(f) \times D(l) \times H(h(f)), \quad (8)$$

where K_{XT} is an empirically-obtained scaling factor, $F(f) = f^p$ with $p \in \mathbb{R}$, $D(l)$ is a function of the coupling length l , and $H(h(f))$ determines the dependency on the insertion loss $h(f)$. In particular, $K_{XT} = K_{\text{FEXT}} = 1.7783 \times 10^{-10}$, $F(f) = f^1$, $D(l) = \sqrt{l}$ and $H(h(f)) = |h(f)|$ for FEXT worst case, whereas $K_{XT} = K_{\text{NEXT}} = 1 \times 10^{-7}$, $F(f) = f^{0.75}$, $D(l) = 1$ and $H(h(f)) = \sqrt{1 - |h(f)|^4}$ for NEXT [15].

Available measurements suggest that intra-quad equal level far-end crosstalk (ELFEXT) magnitude, i.e., channel insertion loss subtracted from FEXT in [dB], is proportional to f^2 in quad-based cables [14]. Therefore, we derive the worst-case ELFEXT magnitude from the model in [15] and use it in a curve fitting analysis of our measurement data set to calculate the value of p_{FEXT} . The same analysis is conducted for NEXT measurements, calculating the intra-quad equal level near-end crosstalk (ELNEXT) magnitude to estimate p_{NEXT} . Then, to obtain the corresponding worst cases, we calculate FEXT and NEXT adding (in [dB]) the channel insertion loss initially subtracted for conducting the curve fitting analysis, and vary the scaling constant K_{XT} until the worst-case criterion, i.e., only 1% of the magnitudes are above the curve, is met. The values of p and K_{XT} for the intra- and inter-quad FEXT and NEXT worst-case models are given in Table I. Figure 1 shows the measured intra-quad FEXT magnitudes of a 50 m A-2Y(L)50×2×0.4 cable (thin colored lines), the ETSI worst-case model [15] (dashed red) and the obtained/fitted worst-case

TABLE I
INTRA- AND INTER-QUAD WORST CASE FEXT AND NEXT PARAMETERS.

Crosstalk	FEXT		NEXT	
	K_{XT}	p	K_{XT}	p
Intra-quad	2.7527×10^{-16}	1.8121	3.3870×10^{-7}	0.7126
Inter-quad	1.7783×10^{-10}	1	1×10^{-7}	0.75

model (thick green). Notice that the ETSI worst-case model intersects the measured data at about 30 MHz, which confirms that it is not valid for frequencies above 30 MHz. On the other hand, our proposed worst-case model reproduces well the measurement data beyond VDSL2 limits, i.e., between 30 MHz and 212 MHz. Consequently, we use this worst-case model and FEXT and NEXT measurements to characterize the random variables $\chi^{FEXT}(f)$ and $\chi^{NEXT}(f)$ to obtain the stochastic models given by (6) and (7). Our characterization approach and results are explained in the following section.

C. Model parameter extraction

We measured FEXT and NEXT transfer functions in a 50 m A-2Y(L)50 \times 2 \times 0.4 binder cable. We statistically characterize the random variables $\chi(f)^{FEXT}$ and $\chi(f)^{NEXT}$ by extracting their mean $\mu_{dB}(f)$ and standard deviation $\sigma_{dB}(f)$ from the FEXT and NEXT magnitudes relative to their corresponding 1% worst-case magnitude for intra-quad and inter-quad pairs. To obtain a tractable model, we selected a representative distribution with frequency-independent values μ_{dB} and σ_{dB} for every relationship. While we note that in practice the distribution of FEXT magnitude is more complex, we deem the Gaussian approximation appropriate for the assessment carried out in this paper. The statistical parameters obtained for inter-quad and inter-quad FEXT and NEXT normalized magnitudes are provided in Table II.

IV. NETWORK CHARACTERIZATION

Obtaining reliable simulation results is in general a difficult task, because it is hard to reproduce the real DSL network. Based on studies of distribution lengths across the world, the work in [7] proposes to use a Gamma distribution with shape parameter $\alpha = 2$ and scale parameter $\beta = 302$ m (mean value $\mu = \beta \times \alpha = 604$ m) as typical length distribution of the DSL access network. However, this distribution is only representative for the length range of fiber-to-the-node (FTTN) networks, one of several fiber-to-the-X-point (FTTX) topologies (FTTX

TABLE II
STATISTICAL PARAMETERS OF THE CHARACTERIZED 50-PAIR BINDER

Relationship	FEXT		NEXT	
	μ (dB)	σ (dB)	μ (dB)	σ (dB)
Intra-quad	4.5	1.9	12.7	5.4
Inter-quad	20	8.6	15.9	6.8

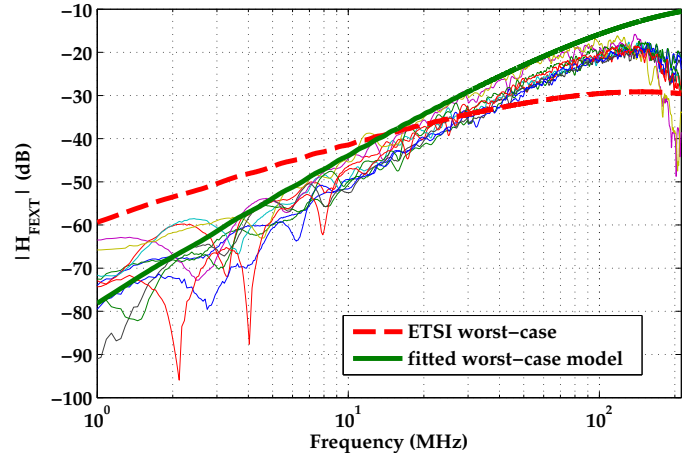


Fig. 1. Intra-quad FEXT magnitude of a 50 m 50-pair binder. Comparison of measured data (thin/colored), ETSI [15] (dashed-red) and fitted worst cases (thick green).

scenarios are detailed in [8], [9]). FTTX are access network topologies that introduce optic links to increase DSL services' data rate by shortening the local loop, so that its attenuation and coupling length are reduced; thus, FTTX topologies differ from each other in the length of the replaced segment, i.e., the common length in which each pair within the binder cable is shortened. We can then assume that the distribution shape α of the proposed Gamma distribution remains unchanged in each FTTX topology, whereas its mean length μ varies, i.e., length distributions are characterized by their scale parameter β . Consequently we define as selecting criterion to obtain suitable β values for each FTTX topology, the symmetric inclusion of each length range (presented in [8], [9]) into 95% of a gamma distribution, i.e., 2.5% of the distribution lengths are shorter than the lower limit and 2.5% are longer than its upper limit. We present in Table III the scale β and mean μ parameters of the Gamma distributions that meet this criterion for Central-Office-based (CO-based), FTTN, FTTC, FTTdp and fiber-to-the-Building (FTTB) topologies. Their cumulative functions are illustrated in figure 2.

V. SIMULATION RESULTS

In this section we show how a thorough numerical analysis can be used to guide standardization efforts aiming at

TABLE III
SCALE β AND MEAN μ FOR GAMMA-DISTRIBUTED FTTX SCENARIOS

Scenario	β (m)	μ (m)
CO-based	1093	2186
FTTN	302	604
FTTC	101	202
FTTdp	50	100
FTTB	20	40

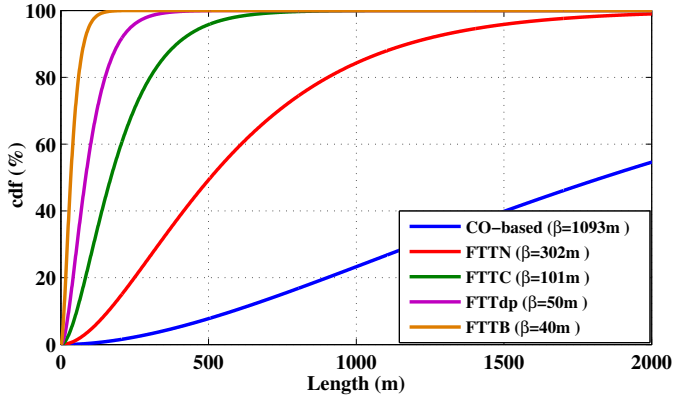


Fig. 2. Cumulative distribution function of Gamma-distributed ($\alpha = 2$) loop lengths for FTTX scenarios.

resolving coexistence problems between G.fast and vectored VDSL2. Considering realistic scenarios in which those two not fully compatible standards actually might exist, we analyze two distinct technological measures to counteract coexistence problems. On one hand, we look at the potential gains that could be achieved by introducing mechanisms for synchronization between co-located G.fast and vectored VDSL2 systems (which may be hard to achieve) and its impact on both systems. On the other hand, we evaluate the role of band plans as simple and effective means to improve spectral compatibility. For each case, we analyze the potential reduction in performance degradation derived from implementing the corresponding mitigation technique. Ultimately, we want to help answer the question whether it is worth considering to introduce these measures, considering the required efforts to do so.

A. Simulation setup and parameters

G.fast is intended to be deployed in FTTdp scenarios [9]. Therefore, we generate loop lengths drawn from the gamma distribution as described in Section IV using the parameters in Table III. The quad-structured 50-binder referred in Section III is considered and its FEXT and NEXT channel functions are modeled using (6) and (7) with random variables χ^{FEXT} and χ^{NEXT} determined by the statistical parameters in Table II. The insertion loss of the direct channel is modeled according

TABLE IV
SIMULATION PARAMETERS

Parameter	Value	
	VDSL2	G.fast
Band plan and mask	998ADE17-M2x-B	106a
Carrier spacing	4.3125 kHz	51.75 kHz
Noise floor	-130 dBm/Hz	-130 dBm/Hz
Shannon gap	10.75 dB	10.75 dB
Efficiency	0.785	0.785
Bitloading cap b_{max}	15 bits	12 bits

to [14, Section B.1.1].

Vectoring is applied on G.fast and VDSL2 transmitted signals by calculating the DPC [13] using the operation in (5). Perfect channel knowledge is assumed. The simulation parameters for the VDSL2 and G.fast systems are summarized in Table IV. For G.fast transmission, we assume symmetric DS/US ratio, i.e., 50% multiplexing time is assigned to downstream and upstream transmission slots.

We consider full binder occupation with $N = 50$ services, where N_g and N_v users are respectively served by G.fast and vectored VDSL2, while $N_g + N_v = N$. To analyze the mutual impact of vectored-VDSL2 and G.fast for different deployment scenarios, three cases are considered. In the first one, $N_g = 10$ G.fast services are jointly deployed with $N_v = 40$ VDSL2 services; this setup intends to reproduce the initial phase of G.fast rollout where G.fast is introduced into a VDSL2-dominated binder, i.e., $N_g < N_v$. The second setup represents a balanced setup; equal number of G.fast and VDSL2 services coexist within the binder, i.e., $N_g = N_v = 25$. In the third case, G.fast is dominant and the inverse VDSL2-dominated configuration is considered, i.e., $N_g = 40$ and $N_v = 10$.

To quantify systems' performance, we use the *percent loss (PL)* defined in [20] as

$$PL = 100\% \cdot \left(\frac{SDR - VDR}{SDR} \right), \quad (9)$$

where VDR is the vectored data rate when the vectoring operation in (5) is applied by each vectoring system, and SDR is the single line data rate.

B. Potential gains of synchronous transmission implementation

First, we analyze the introduction of G.fast without spectral constraints, i.e., G.fast uses the frequency range between 2.2 MHz and 106 MHz [1]. Figure 3 shows the mean downstream percent loss (PL) with respect to the line length, i.e., the reach-percent-loss curve, for G.fast-dominated, balanced and VDSL2-dominated scenarios. We evaluate the two possible symbol alignments [11]: full alignment [11, eq.(5), eq.(12)] (solid) and worst-case alignment [11, eq.(7), eq.(16)] (dashed). Full symbol alignment represents a potential coordinated transmission between VDSL2 and G.fast systems, i.e., synchronous transmission, whereas worst-case alignment constitutes the lower performance boundary due to inter-system asynchronous transmission. We start by analyzing the later alignment scenario. The triangles in Figure 3b indicate the minimum loop length at which the PL of VDSL2 is lower or equal than G.fast's PL. Notice that in the best scenario for VDSL2, i.e., VDSL2-dominated, this point occurs at 120m, which corresponds to the 70th percentile of the gamma distribution defined in Section IV. Thus, it is estimated that 70% of the VDSL2 systems will obtain in average lower performance than coexisting G.fast systems in the most favorable scenario for VDSL2. The same analysis conducted in the other two scenarios yields higher percents of under-performing VDSL2 systems in

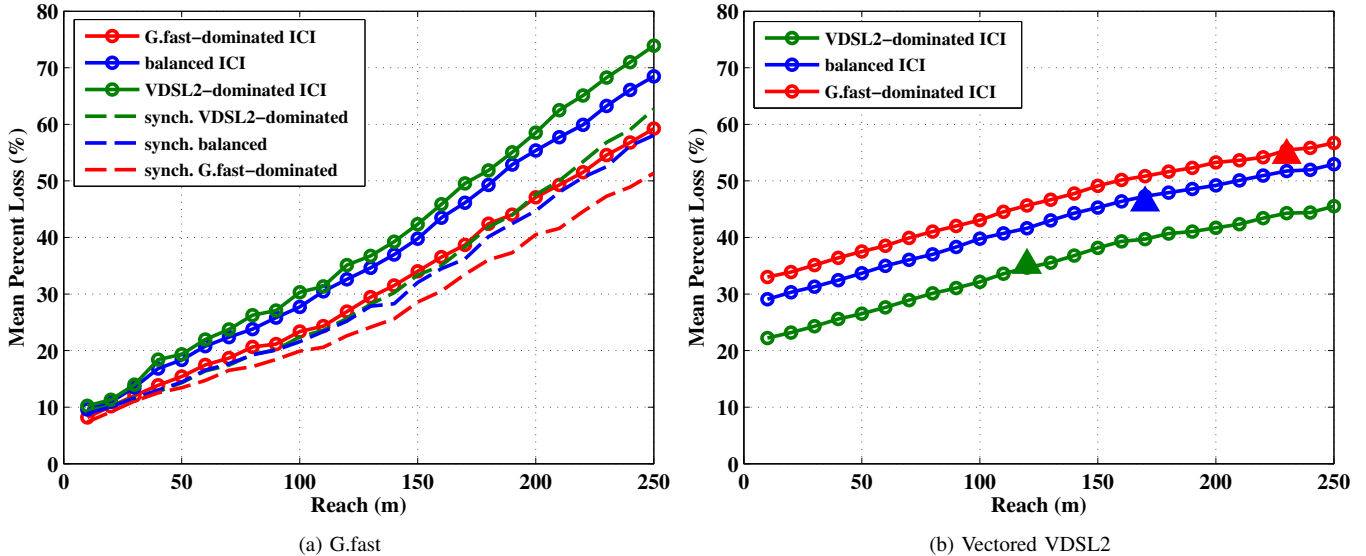


Fig. 3. Mean downstream Percent Loss (PL) (9) for balanced, G.fast-dominated and VDSL2-dominated cases under worst-case ICI (solid) and synchronous transmission (dashed). Figure (a) shows G.fast performance. Figure (b) depicts the results for vectored VDSL2; its synchronous transmission values overlap worst-case ICI results and are not shown. The triangles indicate the minimum length at which VDSL2’s PL is equal or lower than in G.fast systems.

comparison with coexisting G.fast services: 85% and 94% in balanced and G.fast-dominated scenarios, respectively. We then conclude that the coexistence of G.fast and vectored VDSL2 has higher impact on vectored VDSL2 than on its counterparts in terms of performance degradation, i.e., PL. Subsequently, we analyze the performance improvements of implementing synchronous transmission between the two coexisting systems under the defined scenarios. Although we do not consider the implementation complexity in our analysis, the obtained results may be assumed as an approach to a potential technique to be considered for mitigating the mutual performance degradation in coexisting environments.

Regarding synchronous transmission (dashed curves in Figure 3), its PL values in vectored VDSL2 systems (Figure 3b) do not exhibit significant difference in comparison with worst-case-aligned transmission and they overlap. Therefore, implementing inter-system synchronous transmission does not entail considerable gains over asynchronous transmission. Conversely, G.fast services degradation is lower when such transmission is implemented: up to 10% less PL is obtained in long loops with respect to the worst-case-aligned transmission. The impact of mitigating the inter-system interference through synchronous transmission is only noticeable in G.fast due to its symbol duration; 12 G.fast’s symbols interfere on each VDSL2 symbol and synchronous transmission only varies the interference of one of them [11], resulting in minimal changes in the total ICI. On the other hand, G.fast systems may be interfered by one (full alignment) or two VDSL2 symbols (partial alignment) [11] and therefore, the difference in the interference levels is noticeable, so synchronous transmissions carriers performance improvements.

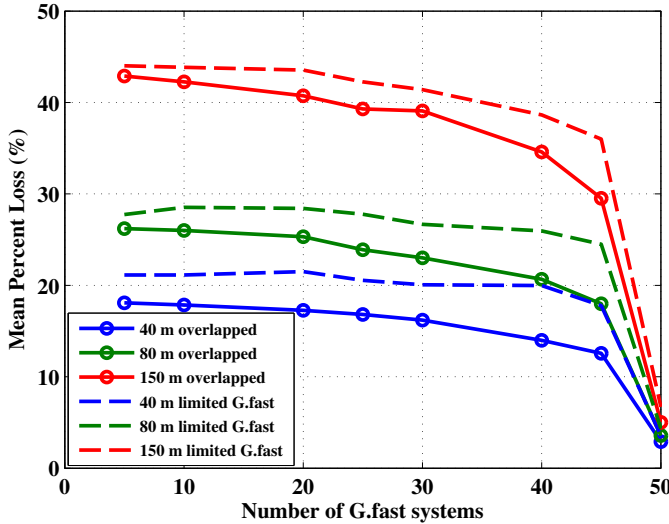
C. Effectiveness of spectral-compatible band plans

The standardization process of G.fast has considered a spectral-compatible profile to mitigate the effects on VDSL2 systems. This profile limits G.fast to use carriers only above 17 MHz. We then analyze the impact of this mitigation technique, referred in this work as *limited-G.fast*.

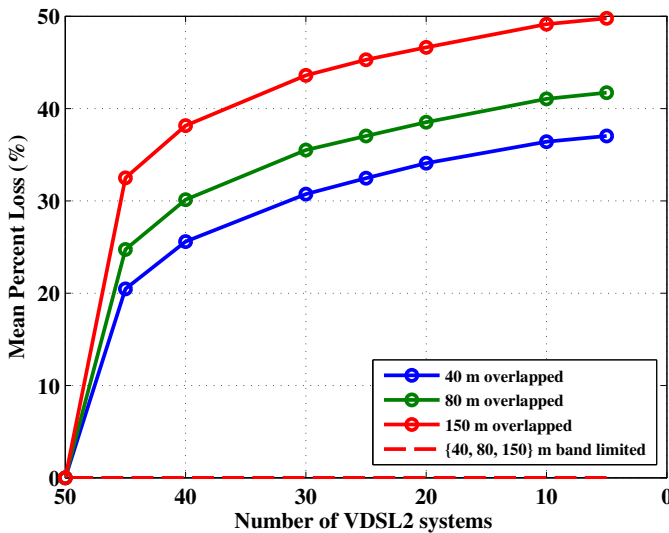
Figure 4 illustrates the PL values of worst-case-aligned systems implementing full-spectrum (solid curves) and spectral-compatible (dashed) profiles, i.e., limited-G.fast, for different number of deployed G.fast/VDSL2 systems. The evaluation is conducted for three representative line lengths: 40 m, 80 m and 150 m. They correspond to the 20th, 50th and 80th percentiles of the DP length distribution, respectively and therefore, their values represent the maximum average PL that can be obtained for the corresponding percentile of lines. The results show that limiting G.fast’ spectrum allows VDSL2 systems to obtain their single line performance. This is derived from the close-to-zero values of the PL shown in Figure 4b for limited G.fast simulations. Although the results also show that its implementation negatively impacts G.fast performance, a maximum degradation of about 5% (obtained for 45 G.fast systems at 40 m) with respect to the full-spectrum implementation indicates that such technique is suitable in coexistence scenarios. Indeed, its deployment in conjunction with synchronous transmission can potentially reduce the impact on G.fast performance.

VI. CONCLUSIONS

Goal of this paper was to analyze the impact of synchronization and spectral-compatible band plans —which potentially might be implemented to resolve coexistence problems between G.fast and vectored VDSL2— and help answer the



(a) G.fast



(b) Vectored VDSL2

Fig. 4. Mean downstream Percent Loss (PL) for different number of (a) G.fast and (b) vectored VDSL2 systems implementing full-spectrum (solid) and spectral-compatible band plans (dashed). The number of VDSL2 systems is inverted in (b) for vertical comparison of corresponding deployment scenarios.

question if these means should be implemented and/or considered further for standardization. In order to achieve this goal, we looked at the important case where G.fast and vectored VDSL2 are jointly operated from the distribution point. To conduct a realistic analysis, we developed FEXT and NEXT channel models for the G.fast frequency range and used a realistic length distribution to reproduce FTTP networks.

A comparative analysis of asynchronous and synchronous transmission between G.fast and VDSL2 shows that introducing synchronization between those systems has a relatively low impact on vectored VDSL2 performance whereas the gains for G.fast are better. At the end, it remains questionable if mechanisms to establish a synchronous transmission between

VDSL2 and G.fast should be explored, especially considering the fact that the implementation of such mechanisms may be hard to realize. On the other hand, the use of spectral-compatible band plans seems to be promising, since the vectored VDSL2 systems are able to nearly achieve their single line performance, while the cost for the G.fast systems is relatively low.

REFERENCES

- [1] *Fast access to subscriber terminals (G.fast) Power spectral density specification*, G.9700, International Telecommunication Union Std., April 2014.
- [2] M. Timmers, M. Guenach, C. Nuzman, and J. Maes, "G.fast: Evolving the copper access network," *IEEE Communications Magazine*, 2013.
- [3] *Very high speed digital subscriber line transceivers 2 (VDSL2)*, Rec. ITU-T G.993.2, International Telecommunication Union Std., December 2011.
- [4] *Self-FEXT cancellation (vectoring) for use with VDSL2 transceivers*, Rec. ITU-T G.993.5, International Telecommunication Union Std., April 2010.
- [5] R. B. Moraes, P. Tsiaflakis, and M. Moonen, "Intercarrier interference in dsl networks due to asynchronous dmt transmission," in *Proc. IEEE International Conference on Acoustics, Speech and Signal Processing (ICASSP)*, 2013.
- [6] V. M. K. Chan and W. Yu, "Multiuser spectrum optimization for discrete multitone systems with asynchronous crosstalk," *IEEE Transactions on Signal Processing*, vol. 55, no. 11, pp. 5425–5435, November 2007.
- [7] J. Maes, M. Guenach, M. B. Ghorbel, and B. Drooghaag, "Managing unvectorized lines in a vectorized group," in *Proc. IEEE Global Communications Conference (GLOBECOM), Symposium on Selected Areas in Communication (SAC)*, Atlanta, GA, USA, December 9–13 2013.
- [8] *Deploying Fiber-To-The-Most-Economic Point (white paper)*. Alcatel-Lucent, 2007.
- [9] R. Strobel, *G.fast Technology and the FTTP Network (white paper)*. Lantiq, October 2014.
- [10] C. Leung, S. Huberman, K. Ho-Van, and T. Le-Ngoe, "Vectored DSL: Potential, implementation issues and challenges," *IEEE Commun. Surveys Tuts.*, vol. 15, no. 4, pp. 1907–1923, Fourth Quarter 2013.
- [11] S. Drakulić, M. Wolkerstorfer, and D. Statovci, "Coexistence analysis of asynchronous digital subscriber lines with different sampling rate and carrier frequency spacing," in *IEEE Global Communications Conference (GLOBECOM)*, 2014.
- [12] G. Ginis and J. M. Cioffi, "Vectored transmission for digital subscriber line systems," *IEEE J. Select. Areas Commun.*, vol. 5, no. 4, pp. 1085–1104, June 2002.
- [13] R. Cendrillon, G. Ginis, E. V. den Bogaert, and M. Moonen, "A near-optimal linear crosstalk precoder for downstream VDSL," *IEEE Trans. Commun.*, vol. 55, pp. 860–863, 2007.
- [14] "Broadband copper cable models," Broadband Forum, Tech. Rep. TR-285. Issue 1, February 2015.
- [15] *Very High Speed digital subscriber line system (VDSL2)*, Technical Specification ETSI TS 101 271, European Telecommunications Standards Institute Std., January 2009.
- [16] M. Sorbara, P. Duvaut, F. Shmulyian, S. Singh, and A. Mahadevan, "Construction of a DSL-MIMO channel model for evaluation of FEXT cancellation systems in VDSL2," in *Proc. IEEE Sarnoff Symposium*, April 2007, pp. 1–6.
- [17] *Multiple-Input Multiple-Output Crosstalk Channel Model*, ATIS-0600024, Alliance for Telecommunications Industry Solutions Std., 2011.
- [18] W. Xu, C. Schroeder, and P. A. Hoeher, "A stochastic MIMO model for far-end crosstalk in VDSL cable binders," in *Proc. IEEE International Conference on Communications (ICC)*, 2009.
- [19] R. Strobel, R. Stolle, and W. Utschick, "Wideband modeling of twisted-pair cables for mimo applications," in *Proc. IEEE Global Communications Conference (GLOBECOM), Symposium on Selected Areas in Communication (SAC)*, Atlanta, GA, USA, December 9–13 2013.
- [20] "Testing of G.993.2 self-FEXT cancellation (vectoring)," TR-249 Issue 1, Broadband Forum, Tech. Rep. TR-249. Issue 1, March 2014.